APH N.S., Heavy Ion Physics **15** (2002) 000–000

HEAVY ION PHYSICS
©Akadémiai Kiadó

Correlated Charged Pions from Chiral Dynamics in High-Energy Nuclear Collisions

Jørgen Randrup

Nuclear Science Division, Lawrence Berkeley National Laboratory,
University of California, Berkeley, California 94720, USA

Received October 11, 2001

Abstract. It is expected that chiral symmetry is approximately restored in the very excited matter produced in a high-energy nuclear collision and that the chiral order parameter will thereafter quickly relax towards its aligned vacuum value. This non-equilibrium evolution of the environment endows the pionic degrees of freedom with a time-dependent effective mass and this agency, in turn, may create correlated soft pions that could provide specific observable signatures of the chiral dynamics that are based solely on charged pions.

Keywords: relativistic heavy-ion collisions, chiral symmetry, pion production
PACS: 25.75.-q,11.30.Rd,05.60.Gg,11.10.-z

1. Introduction

High-energy nuclear collisions are expected to produce transient systems within which chiral symmetry is approximately restored and the matter is partially deconfined. The identification and exploration of such a novel phase of matter is currently a major experimental goal and the efforts have intensified with the recent commisioning of the Relativistic Heavy Ion Collider at BNL [1].

Through the past decade, it has been speculated that the rapid expansion of the collision zone, after an approximate restoration of chiral symmetry has occurred, may produce long-wavelength isospin-polarized agitations of the pionic field, commonly referred to as *disoriented chiral condensates* (DCC), which in turn should lead to anomalies in the resulting pion multiplicity distribution [2–4].

Initially the focus was on the expected broadening in the distribution of the neutral pion fraction (the number of neutral pions divided by the total number), but experimental searches for such a signal have yielded a null result [5,6]. However, it has become increasingly clear from model calculations that any DCC effect is carried

1219-7580/01/ $ 5.00

exclusively by relatively soft pions and thus the signal may be overwhelmed by the background unless the analysis is limited to the soft pions. Moreover, the neutral pions decay into photon pairs and since a reconstruction is practically impossible, the neutral pion fraction is less than ideal as an experimental indicator.

Furtunately, as breifly discussed below, recent detailed dynamical calculations suggest that there may be suitable signals that are based exclusively on the charged pions and which would therefore better lend themselves to experimental detection.

2. Field simulations for Bjorken rods

In order to get an idea of how the physical environment may evolve after the initial violent collision stage, it is instructive to consider a system endowed with a Bjorken scaling expansion in the direction of the incident relative motion (in order to account roughly for the dominant longitudinal expansion) and, for simplicity, assume that the system has axial symmetry. Thus, such a model system appears as a stretching rod and it may therefore be referred to as a *Bjorken rod*, as illustrated in Fig. 1.

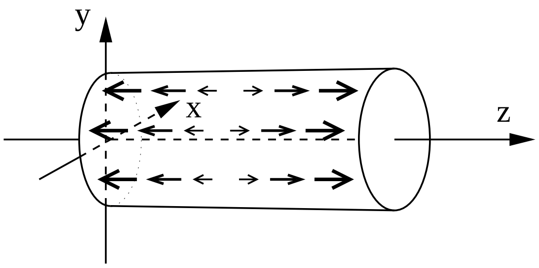

Fig. 1. Schematic representation of a *Bjorken rod*: an axially symmetry system endowed with a longitudinal Bjorken scaling expansion.

The semi-classical linear σ model [7] offers a simple tool for exploring the principal features of the chiral degrees of freedom, both in thermal equilibrium [7,8] and for the rapidly evolving environments formed in high-energy collisions [9,10]. For Bjorken-type systems, it is convenient to employ the comoving variables (τ, η) in place of (t, z), where $t = \tau \cosh \eta$ and $z = \tau \sinh \eta$, and the equation of motion for the O(4) chiral field $\boldsymbol{\phi}(\boldsymbol{r}, t) = (\sigma, \boldsymbol{\pi})$ is then relatively simple,

$$\left[\frac{\partial^2}{\partial_\tau^2} - \frac{\partial^2}{\partial_x^2} - \frac{\partial^2}{\partial_y^2} - \frac{1}{\tau^2}\frac{\partial^2}{\partial_\eta^2} + \lambda(\boldsymbol{\phi} \circ \boldsymbol{\phi} - v^2)\right] \boldsymbol{\phi} \;=\; H\hat{e}_\sigma - \frac{1}{\tau}\frac{\partial}{\partial_\tau}\boldsymbol{\phi} \;. \tag{1}$$

Once the chiral field $\boldsymbol{\phi}(\boldsymbol{r})$ (including its time derivative $\dot{\boldsymbol{\phi}}(\boldsymbol{r})$) has been suitably initialized [11,12], its time evolution can be determined by elementary numerical means, employing a simple leap-frog method of propagation [7,9,12].

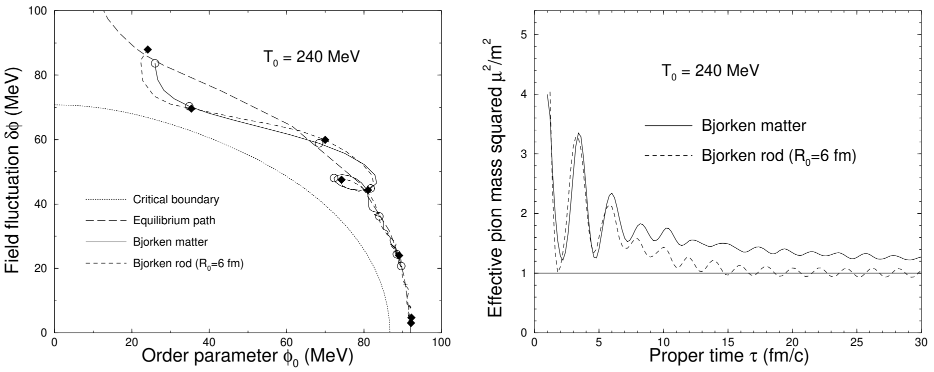

Fig. 2. *Left-hand panel:* The phase evolution of the interior region of a Bjorken rod with an intial bulk temperature of $T_0 = 240$ MeV and an initial transverse radius of $R_0 = 6$ fm, together with the results for the corresponding Bjorken matter (for which $R_0 \to \infty$); also shown are the adiabatic path (going through the thermal equilibria) and the critical boundary (inside which the field is supercritical so the softest pionic modes are unstable). *Right-hand panel:* The corresponding evolutions of the effective pion mass μ (in the bulk region). (From Ref. [12].)

It is instructive to first consider how the the interior region evolves on the chiral phase diagram. Because of the non-equilibrium character of the dynamics, the phase diagram is most conveniently represented directly in terms of the chiral field, using the local average field strength ϕ_0 as the order parameter and the associated local field fluctuation $\delta\phi$ as the measure of the agitation [7–9]. As illustrated on the left in Fig. 2, the system stays well away from the supercritical region, but exhibits significant quasi-regular oscillations around the equilibrium path (which displays the familiar cross-over from a chirally aligned phase at low temperature towards a chirally symmetric phase at high temperature). Moreover, at early times the interior of the rod behaves as the corresponding *Bjorken matter* (a Bjorken rod with infinite radius), while the relaxation proceeds significantly faster later on, due to the transverse expansion (which is absent in matter).

This behavior is then reflected in the effective pion mass $\mu(\boldsymbol{r},t)$ which is given in terms of the local order parameter and the local field fluctuations. For example, the mass of the neutral pion is given by

$$\mu^2(\boldsymbol{r},t) \;=\; \lambda\left[\phi_0(\boldsymbol{r},t)^2 + \delta\phi^2(\boldsymbol{r},t) + 2\delta\pi_0^2(\boldsymbol{r},t) - v^2\right] \;. \tag{2}$$

The resulting time evolutions are depicted on the right in Fig. 2. It is important to note that although the approach of the effective mass to its free value m is faster in the rod scenario, persistent oscillations around m remain present for a long time, thus providing a mechanism for amplification of frequency-matched pionic modes.

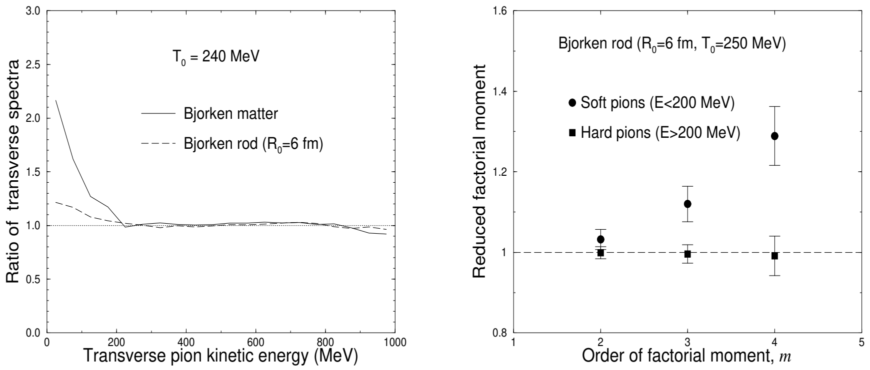

Fig. 3. *Left-hand panel:* The ratio between the final transverse pion spectrum, $d^3N/d^2\boldsymbol{p}_\perp dy$, and the associated equilibrium spectrum obtained by fitting the dynamical result with a Bose-Einstein form within the "hard" energy interval 200-1000 MeV, for a longitudinally expanding rod (dashed curve) having an initial radius of $R_0 = 6$ fm and with an initial bulk temperature of $T_0 = 240$ MeV, as well as the corresponding result for Bjorken matter. *Right-hand panel:* The reduced factorial multiplicity moments $\langle N(N-1)\cdots(N-m+1)\rangle/\langle N\rangle^m$ obtained for a sample of rods prepared with $R_0 = 6$ fm and $T_0 = 250$ MeV, as a function of the order m, for either soft (dots) or hard (squares) pions. (From Ref. [12].)

Such simulations have identified a number of simple candidate observables [12]. One is the transverse spectral profile which is expected to exhibit a marked enhancement below $m_\perp \approx 200$ MeV due to the parametric amplification by the time modulation of the mass, as illustrated in Fig. 3 (left). However, additional sources of soft pions may render any observed effect less specific. A more promising candidate observable is the fluctuation in the multiplicity of soft pions which was found to display a significant anomalous increase with the order of the correlation, as shown in Fig. 3 (right). Since a subsequent study [13] has shown that such an effect is absent in both RQMD and HIJING (both widely used event generators using only conventional physics input), it it appears that this observable has a larger specificity and hence it may be worthwhile to pursue it in the data analysis. The azimuthal structure of the pion emission pattern, as encoded in the corresponding multipole strength function, may also be informative.

When seeking to make contact with data, it should be kept in mind that the calculations involve a number of approximations and idealizations. Therefore, the theoretical results are not directly comparable with experimental data, but should rather serve to direct the attention to the possible presence of the various specific signals. Generally speaking, our studies suggest that while one should not expect spectacular DCC signals, carefully designed quantitative analyzes might bring out any anomalous DCC-type behavior in the data.

3. Pion pair correlations

In recognition of the key feature that the basic production mechanism creates neither momentum nor charge, it was recently suggested that an especially attractive signature may exist in the form of an approximately back-to-back correlation between oppositely charged soft pions [14]. In order to most clearly bring out the basic mechanism, we consider first the simple case where the environment, and hence the effective mass, is spatially uniform, as is approximately the case in the interior of the collision zone. It is then obvious that although the time dependence of the mass may generate considerable agitation, this agency cannot add any net momentum. Therefore, the any pions produced by the mechanism must be formed pairwise and moving in opposite directions. Furthermore, by a similar reasoning, the time dependence of the mass does not add any charge, so the produced pairs must be oppositely charged. Thus, the particles generated by an arbitrary time dependence in a uniform medium are charge-conjugate back-to-back pairs. This basic feature may be exploited as a probe of the chiral dynamics.

3.1. Uniform environment

The spatially uniform scenario is particularly simple to treat because the Hamiltonian decouples so that each degenerate pair of oppositely moving modes can be considered separately. A quantum-field treatment is then relatively simple [15]. The eigenmodes for any given value of the effective mass μ_0 can be obtained by a suitable squeezing of the standard free modes. Since these modes (which we shall denote as *quasiparticles*) diagonalize the problem for the particular value of μ_0, they provide a particularly instructive basis for the analysis of the evolution.

We use $\hat{A}_{\mathbf{k}}$ to denote the annihilation operator for the quasiparticle modes corresponding to the instantaneous value of the effective mass, $\mu_0(t)$. The Heisenberg representation of the corresponding time-dependent quasiparticle mode is then

$$\hat{\mathcal{A}}^{\nu}_{\mathbf{k}}(t) \;=\; \mathcal{U}_k(t)\hat{A}^{\nu}_{\mathbf{k}} \;+\; \mathcal{V}_k(t)^*(\hat{A}^{\bar{\nu}}_{-\mathbf{k}})^{\dagger}\ . \tag{3}$$

Here the subscript $\mathbf{k}$ denotes the wave number and the superscript $\nu=\pm$ denotes the charge state (with $\bar{\nu}\equiv-\nu$). The time dependence of the quasiparticle operators $\hat{\mathcal{A}}^{\nu}_{\mathbf{k}}(t)$ derive both from the usual Heisenberg evolution and from the continual redefinition of the quasiparticle basis. The Bogoliubov coefficients $\mathcal{U}_k(t)$ and $\mathcal{V}_k(t)$ are given in terms of the corresponding mode functions which in turn are determined by the equation of motion for the pion field. Being dependent only on the mode frequency ω_k, they are the same for all charge components ν and for all momenta with the same magnitude $p{=}\hbar k$. We note that the time evolution mixes particle states of forward-going positive pions with hole states of backward-going negative pions, a reflection of the key conservation properties.

Let us now for simplicity assume that the system can initially be described as a thermal ensemble. The corresponding occupancy of a given initial quasiparticle mode is then $N_k = 1/[\exp(\omega_k/T_0)+1]$, where T_0 is the specified temperature. The expected occupancy of the mode at a later time t readily follows from (3),

$$N_{\mathbf{k}}^{\nu}(t) \;\equiv\; \langle t|\hat{N}_{\mathbf{k}}^{\nu}|t\rangle \;\equiv\; \langle t_i|\hat{\mathcal{A}}_{\mathbf{k}}^{\nu}(t)^{\dagger}\hat{\mathcal{A}}_{\mathbf{k}}^{\nu}(t)|t_i\rangle \;=\; |\mathcal{U}_k(t)|^2 N_k + |\mathcal{V}_k(t)|^2(N_k+1)\ . \quad (4)$$

With a bit more elementary operator algebra, it is possible to obtain the following two equivalent expressions for the quasiparticle correlation coefficient,

$$\begin{aligned}
&\sigma_{\mathbf{k}'\mathbf{k}}^{\nu'\nu}(t) \;\equiv\; \langle t|\hat{N}_{\mathbf{k}'}^{\nu'}\hat{N}_{\mathbf{k}}^{\nu}|t\rangle \;-\; N_{\mathbf{k}'}^{\nu'}(t)N_{\mathbf{k}}^{\nu}(t)\\
=\;& N_k\bar{N}_k\ \delta_{\nu'\nu}\delta_{\mathbf{k}'\mathbf{k}} + |\mathcal{U}_k(t)|^2|\mathcal{V}_k(t)|^2 \times (2N_k+1)^2\left[\delta_{\nu'\nu}\delta_{\mathbf{k}'\mathbf{k}} + \delta_{\nu'\bar{\nu}}\delta_{\mathbf{k}',-\mathbf{k}}\right] \quad (5)\\
=\;& N_{\mathbf{k}}(t)\bar{N}_{\mathbf{k}}(t)\ \delta_{\nu'\nu}\delta_{\mathbf{k}'\mathbf{k}} \;+\; |\mathcal{U}_k(t)|^2|\mathcal{V}_k(t)|^2\,(2N_k+1)^2\,\delta_{\nu'\bar{\nu}}\delta_{\mathbf{k}',-\mathbf{k}}\ . \quad (6)
\end{aligned}$$

In the first relation, the term $N\bar{N}$ is the initial Bose-Einstein autocorrelation for the occupancy of the given mode while the second term is the additional correlation introduced by the time dependence of the effective mass, $\mu_0(t)$, and its specific form reflects the fact that the autocorrelation is increased in concert with the back-to-back correlation between charge-conjugate pairs. The last relation shows that the resulting autocorrelation still has the familiar Bose-Einstein form, $N(t)\bar{N}(t)$.

These features are illustrated in Fig. 4. In order to emulate a uniform, longitudinally expanding environment, we use a simple time dependence of the effective mass, $\mu_0^2(t) = m^2 + (\mu_i^2 - m^2)\exp(-t/t_0)[1+\cos(\omega_{\rm osc}t)]/2$, shown in the left panel of Fig. 4. With μ_i=$2m$, t_0=5 fm/c, and $\omega_{\rm osc}$=m_σ, this expression approximates the evolution shown in Fig. 2 from an initial environment where the chiral order parameter is equal to $\langle\bar{q}q\rangle \approx 26$ MeV, corresponding to an initial temperature of $T_0 \approx 240$ MeV in the semi-classical linear σ model [12].

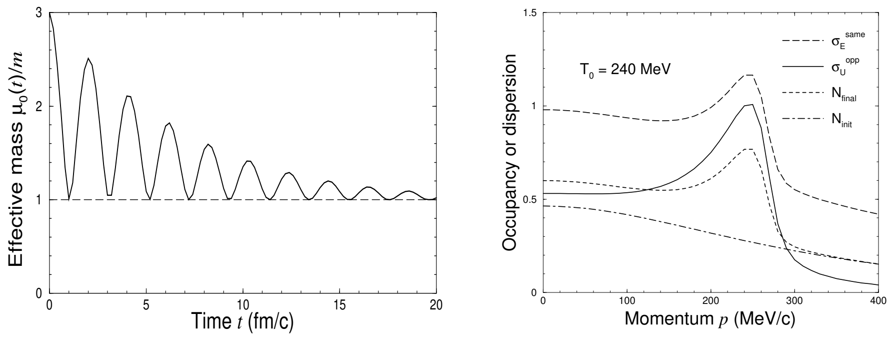

Fig. 4. *Left-hand panel:* The time dependence of the the effective mass function used in the illustration, $\mu_0(t)$. It has a rough correspondence with typical mass functions obtained in dynamical studies with the linear σ model (see Fig. 2). *Right-hand panel:* The resulting amplification and correlation obtained for the mass function $\mu_0(t)$ emulating a uniform expanding scenario. (From Ref. [16].)

Figure 4 (right) shows how the initial Bose-Einstein quasiparticle occupation numbers $N_{\rm init}$ (dot-dashed) are being enhanced below $\approx$300 MeV/c (short dashes). The resulting peak structure in $N_{\rm final}$ is a reflection of the regularity of the order parameter oscillations: particular amplification is experienced by the modes that have their frequency ω_k in the neighborhood of half the σ mass, corresponding to $p \approx 260$ MeV/c for $m_\sigma = 600$ MeV/c^2. The autocorrelation in the mode occupancies (long dashes) exhibits a similar structure (since it is given by $N\bar{N}$). It is noteworthy that although the correlation between oppositely moving charge-conjugate pion pairs (solid curve) is generally smaller than the autocorrelation, as Eq. (5) dictates, it acquires a comparable magnitude in the region of strongest amplification (where the dynamically produced pions dominate over those originally present). On the other hand, this correlation quickly subsides above $\approx$300 MeV/c, bringing out the fact that the effect is confined to the soft regime.

3.2. Non-uniform scenario

Rather than an entirely uniform environment, it would be more realistic to consider a mass function that deviates from the free value only within a finite volume representing the agitated region. When the environment has a spatial dependence, the pions experience forces which tend to erode the pure back-to-back correlation pattern. To ascertain the importance of this effect, it is instructive to consider a simple one-dimensional scenario in which the effective mass function has a diffuse spatial profile, dropping from its central value $\mu_0(t)$ to its free value m according to a Woods-Saxon like modulation, as depicted on the left in Fig. 5.

It was recently shown how the quantum-field treatment of Ref. [15] can be extended to non-uniform scenarios as well, still within the effective mass approximation [16]. The spatial correlation function can then be expressed as follows,

$$\begin{aligned} \rho(\boldsymbol{r},\boldsymbol{r}';t) \;&\equiv\; \langle t|\hat{A}^\dagger(\boldsymbol{r})\hat{A}(\boldsymbol{r}')|t\rangle \;=\; \langle t_i|\hat{\mathcal{A}}^\dagger(\boldsymbol{r},t)\hat{\mathcal{A}}(\boldsymbol{r}',t)|t_i\rangle \\ =\; \rho^{\rm qu}(\boldsymbol{r},\boldsymbol{r}';t)+\rho^{\rm cl}(\boldsymbol{r},\boldsymbol{r}';t) \;&=\; \sum_{\mathbf{L}} \mathcal{V}^{\mathbf{L}}(\boldsymbol{r},t)\mathcal{V}^{\mathbf{L}}(\boldsymbol{r}',t)^* + \rho^{\rm cl}(\boldsymbol{r},\boldsymbol{r}';t)\;, \end{aligned} \tag{7}$$

and the one-body density matrix in the $\mathbf{k}$ representation is given analogously,

$$\begin{aligned} \rho_{\mathbf{kk}'}(t) \;&\equiv\; \langle t|\hat{A}^\dagger_{\mathbf{k}}\hat{A}_{\mathbf{k}'}|t\rangle \;=\; \langle t_i|\hat{\mathcal{A}}^\dagger_{\mathbf{k}}(t)\hat{A}_{\mathbf{k}'}(t)|t_i\rangle \\ =\; \rho^{\rm qu}_{\mathbf{kk}'}(t)+\rho^{\rm cl}_{\mathbf{kk}'}(t) \;&=\; \sum_{\mathbf{L}} \mathcal{V}^{\mathbf{L}}_{\mathbf{k}}(t)\;\mathcal{V}^{\mathbf{L}}_{\mathbf{k}'}(t)^* \;+\rho^{\rm cl}_{\mathbf{kk}'}(t)\;. \end{aligned} \tag{8}$$

In these expressions, the first term arises from the quantum fluctuations in the initial state, while the second term is caused by the real agitations in the initial state (the "classical" or "thermal" field fluctuations). We recall that the quasiparticle annihilation (Schrödinger) operators $\hat{A}$ are defined with respect to the instantaneous eigenbasis (which changes continually due to the time dependence of $\mu(\boldsymbol{r})$) and that $\hat{\mathcal{A}}(t)$ denote the corresponding Heisenberg operators, while the appropriate Bogoliubov coefficients are denoted by $\mathcal{U}(t)$ and $\mathcal{V}(t)$ (see Ref. [16] for details).

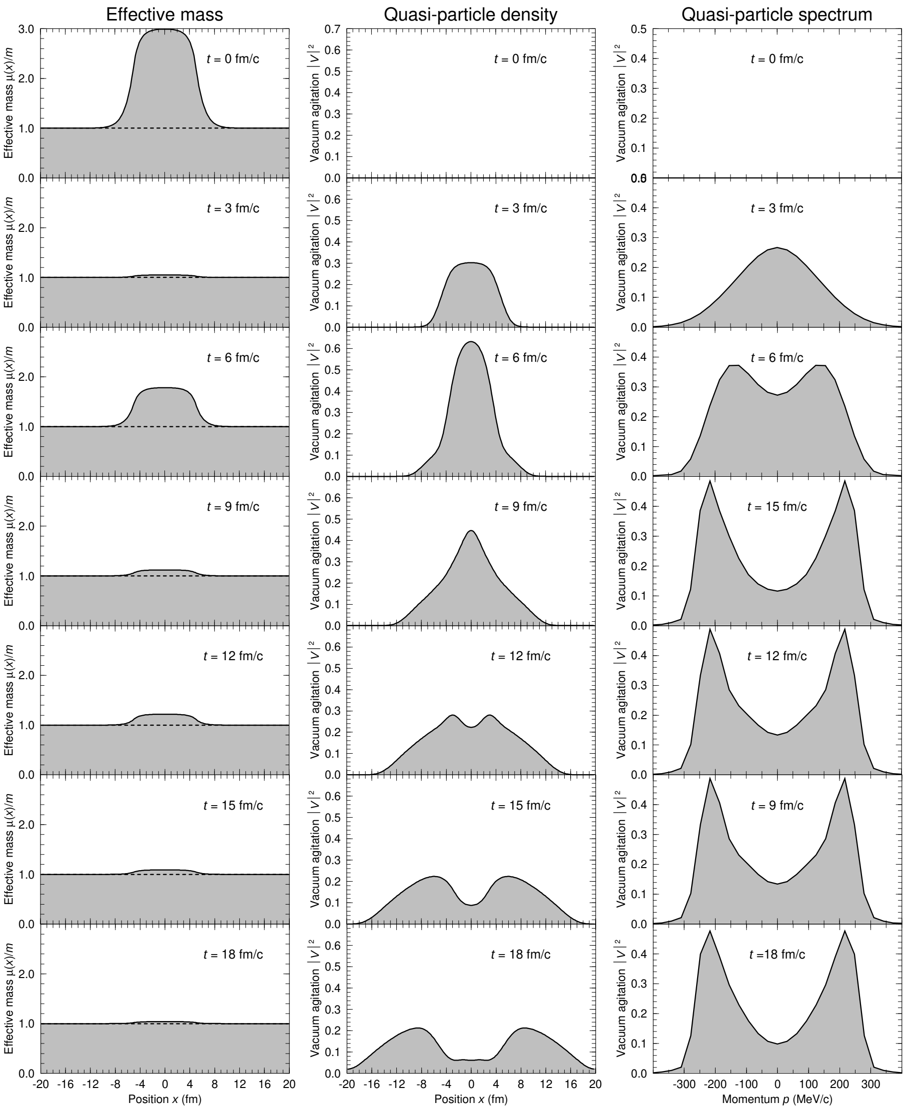

Fig. 5. The spatial density (center) and the spectral distribution (right) of the quasiparticles at successive times t (indicated in fm/c), starting at $t = 0$ from the correlated vacuum associated with the idealized mass function shown on the left.

Figure 5 illustrates the evolution of the diagonal parts of the quantal terms in the above quantities, namely the spatial quasiparticle density and the corresponding spectral profile arising soley from the dynamical agitation of the vaccum,

$$\rho^{\rm qu}(\boldsymbol{r},t) \equiv \rho^{\rm qu}(\boldsymbol{r},\boldsymbol{r},t) = \sum_{\mathbf{L}} |\mathcal{V}^{\mathbf{L}}(\boldsymbol{r},t)|^2 \ , \quad \rho^{\rm qu}_{\mathbf{k}}(t) \equiv \rho^{\rm qu}_{\mathbf{kk}}(t) = \sum_{\mathbf{L}} |\mathcal{V}^{\mathbf{L}}_{\mathbf{k}}(t)|^2 \ . \quad (9)$$

Further contributions will then arise from the amplification of any real quasiparticle agitations that are present initially.

At the initial time, $t = t_i$, the quantities $\rho^{\rm qu}(\boldsymbol{r})$ and $\rho^{\rm qu}_{\mathbf{k}}$ vanish by design. But soon, as the effective mass experiences its first rapid decrease, energy stored in the high initial mass is liberated and a rapidly rising quasiparticle density appears with a spatial profile resembling that of the mass excess $\delta\mu(\boldsymbol{r}) = \mu(\boldsymbol{r}) - m$. Part of these quasiparticles are reabsorbed when the mass again increases and this cycle is repeated in a less noticable manner, as the mass oscillations proceed with an ever decreasing amplitude. The quasiparticles produced by this mechanism have a rather structureless spectrum of approximately gaussian form.

Meanwhile, the regularity of the temporal oscillations in the mass function begins to manifest itself and, at somewhat later times, the spectral profile exhibits a visible enhancement of the modes near the resonance frequency, $\omega_{\rm res} \approx \frac{1}{2}\omega_\sigma =$ 300 MeV, corresponding to a momentum of $p_{\rm res} \approx 266$ MeV$/c$. As a consequence, the quasiparticle gas begins to resemble two countermoving beams with the corresponding flow velocities centered around $v_{\rm flow} \approx \pm p_{\rm res}/m$. The two corresponding outwards bursts are clearly visible at late times when the mass function has largely relaxed to its free form and the production processes have subsided. It is important to recognize that in each individual pion-pair emission process it is entirely random whether a given partner (*e.g.* the positive one) goes forwards or backwards. Thus no overall charge separation occurs, but whenever one pion is emitted in one direction then its partner is emitted (approximately) oppositely.

In order to explore this effect further, one may consider the corresponding two-body correlation function, which can also be obtained within the treatment. The result is illustrated in Fig. 6 (left). As expected, the sharp correlation pattern associated with a uniform system (see Eqs. (5-6)) has become somewhat eroded, due to the spatial dependence of the mass function, but the basic structure largely persists. Thus there is reason to hope that it may be experimentally observable.

In practice, when making an observation, it is not possible to identify a single quantum mode $\mathbf{k}$. Rather, a collection is made over a phase-space domain that encompasses many individual modes. In that situation, one may define the appropriate *coarse-grained* particle number operator, $\hat{\mathcal{N}}^\nu_{\mathcal{K}} = \sum_{\mathbf{k}\in\mathcal{K}} \hat{N}^\nu_{\mathbf{k}}$, where $\mathcal{K}$ denotes a certain domain of $\mathbf{k}$ values. The associated coarse-grained correlation coefficient is then of the form

$$\Sigma^{\nu'\nu}_{\mathcal{K}'\mathcal{K}} \ \equiv \ \langle \hat{\mathcal{N}}^{\nu'}_{\mathcal{K}'} \hat{\mathcal{N}}^{\nu}_{\mathcal{K}} \rangle \ - \ \langle \hat{\mathcal{N}}^{\nu'}_{\mathcal{K}'} \rangle \langle \hat{\mathcal{N}}^{\nu}_{\mathcal{K}} \rangle \ . \quad (10)$$

To examine the effect of such a coarse graining, we let $\mathcal{K}$ encompass all positive pions moving forward with a momentum up to p_0 while $\mathcal{K}'$ includes all negative pions moving backward with a momentum down to $-p_0$.

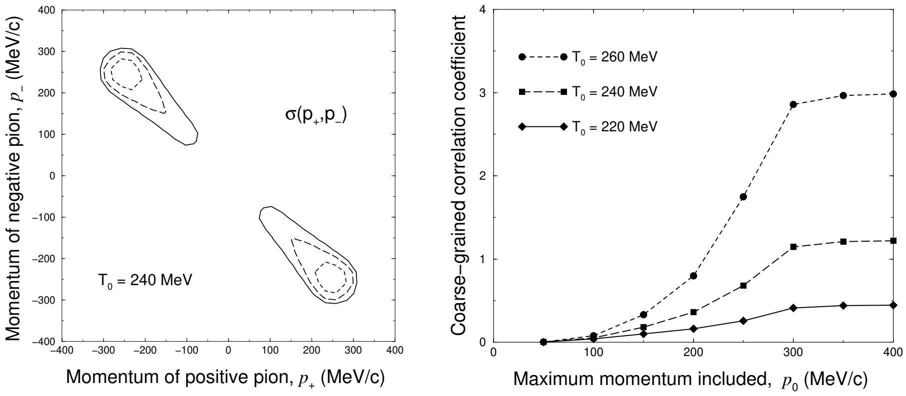

Fig. 6. *Left-hand panel:* Contours (separated by factors of two) of the correlation coefficient for pion pairs of opposite charge as a function of the final momenta, for the one-dimensional scenario considered in Ref. [16] (which uses a space and time dependent effective mass emulating the results obtained in Ref. [12] for the expansion of a system with the initial temperature of $T_0 = 240$ MeV and a initial radius of $R_0 = 5$ fm.) *Right-hand panel:* The coarse-grained correlation coefficient for oppositely moving charge-conjugate soft pions as a function of the cut-off momentum p_0, for three different initial temperatures T_0. (From Ref. [16].)

Figure 6 (right) shows the resulting coarse-grained correlation coefficient for three scenarios corresponding to different initial degrees of agitation and restoration. In all cases the coarse-grained correlation coefficient saturates once the cut-off p_0 is above $\approx$300 MeV/c, the maximum momentum for which the amplification mechanism is effective. Thus there is no gain in signal by extending the cut-off to higher values, while the background increases. In fact, in order to reduce contamination from ρ decays (see below), it may be desirable to employ a momentum cut-off below 300 MeV/c and the results suggest that this might well be possible. In the other direction, at the lower momenta, it is practically difficult to measure pions with $p_\perp$ much below 100 MeV/c but these are seen to contribute relatively little to the total signal.

Another important feature brought out in Fig. 6 (right) is the good sensitivity of the signal to the physical scenario. For the relatively moderate range of initial temperatures considered, $T_0 = 220, 240, 260$ MeV, the initial chiral order parameter takes on the values $\langle \bar{q}q \rangle = 19, 26, 42$ MeV and these differences have become magnified in the resulting correlation signal. This feature demonstrates that the signal is in fact quite sensitive to the degree of chiral restoration achieved early on.

4. Discussion

The initial violent collision of two approaching nuclei is followed by a rapid expansion, which at first proceeds primarily in the longitudinal direction and then only gradually builds up transversly as well. The chiral degrees of freedom then experience an environment that is changing accordingly. Thus one expects that chiral symmetry is approximately restored within the highly excited collision zone early on, but that the chiral order parameter then exhibits a non-equilibrium evolution as it relaxes towards its vacuum value f_π. Since the effective pion mass depends on the chiral order parameter, as well as on the degree of agitation, it is expected to display an overall decay that evolves from its initial high thermal value towards the free mass in an oscillatory fashion reflecting the oscillations of the order parameter. It is therefore natural to investigate whether such a situation may give rise to observable effects, particularly in the charged pions which are the most directly measurable, It is towards this issue that the present note is directed.

Various studies suggest that the oscillatory approach of the order parameter to its finite vacuum value leads to the production of correlated soft pions. Specifically, this mechanism produces a spectral enhancement below $p_\perp \approx 300$ MeV and the associated multiplicity distribution will be anomalously clumpy. In addition, and perhaps most importantly, one would expect these additional pions to exhibit an approximately back-to-back correlation between soft charge-conjugate pairs, a relatively specific signal that may be readily identifiable in the analysis.

However, it should be expected that this signal is partially obscured or eroded by a number of other processes and thus any attempt to extract it from the experimental data must take careful account of such background contributions. One concern is the possible degradation of the primary signal in the course of the propagation of the pions as they leave the interaction zone. Fortunately, as in the "Baked Alaska" scenario discussed by Bjorken [4], the signal-carrying pions appear only relatively late and are moving slowly, so they will have little chance of catching up with the expanding shell of regular collision debris and they may therefore propagate to the detector relatively undisturbed. Another concern is the possible presence of other agencies that may lead to a similar signal. Most important is the decay $\rho \to \pi^+\pi^-$ but, although the two pions are back-to-back correlated, they emerge from a ρ meson at rest with momenta that are somewhat above the upper limit of the interest ($\approx$300 MeV) or, if the decaying ρ is moving, at most one of the daughter pions may be below this limit. It should also be noted that while $\eta(550)$ and $\omega(780)$ may contribute $\pi^+\pi^-$ pairs, these arise in three-body decays which renders them only rather weakly correlated.

Therefore, it appears reasonable to suggest that the current RHIC data be analyzed for indications of large-angle correlation of soft charge-conjugate pion pairs. It may also be worthwhile to scrutinize existing SPS data for such a signal. If indeed identified, this signature may offer a means for probing the degree of chiral restoration achieved initially and the subsequent chiral relaxation dynamics.

This work was supported by the Director, Office of Energy Research, Office of High Energy and Nuclear Physics, Nuclear Physics Division of the U.S. Department of Energy under Contract No. DE-AC03-76SF00098.

References

1. Proceedings of the Fifteenth International Conference on Ultra-Relativistic Nucleus-Nucleus Collisions: Quark Matter 2001, *Nucl. Phys.* **A000** (2002) 1.
2. K. Rajagopal, in *Quark-Gluon Plasma 2*, Ed. R. Hwa, World Scientific (1995).
3. J.-P. Blaizot and A. Krzywicki, *Acta Phys. Polon.* **B27** (1996) 1687.
4. J.D. Bjorken, *Acta Phys. Polon.* **B28** (1997) 2773.
5. T. Brooks *et al.* (MiniMax Collaboration), *Phys. Rev.* **D61** (2000) 032003.
6. T.K. Nayak *et al.* (WA98 Collaboration), *Nucl. Phys.* **A663** (2000) 745.
7. J. Randrup, *Phys. Rev.* **D55** (1997) 1188.
8. J. Randrup, *Heavy Ion Phys.* **13** (2001) 229.
9. J. Randrup, *Phys. Rev. Lett.* **77** (1996) 1226.
10. J. Randrup, *Nucl. Phys.* **A616** (1997) 531.
11. J. Randrup, *Phys. Lett.* **B435** (1998) 251.
12. T.C. Petersen and J. Randrup, *Phys. Rev.* **61** (2000) 024906.
13. M. Bleicher, J. Randrup, R. Snellings, and X.N. Wang, *Phys. Rev.* **C62** (2000) 041901.
14. J. Randrup, *Phys. Rev.* **C63** (2001) 061901.
15. J. Randrup, *Heavy Ion Phys.* **9** (1999) 289.
16. J. Randrup, *Phys. Rev.* **C62** (2000) 064905.